Embryonic development of skull bones in the Sahara horned viper (*Cerastes cerastes*), with new insights into structures related to the basicranium and braincase roof

Eraqi R. Khannoon[1,2], Joni Ollonen[3] and Nicolas Di-Poï[3]

[1]Biology Department, College of Science, Taibah University, Al-Madinah Al-Munawwarah, 344, Saudi Arabia

[2]Zoology Department, Faculty of Science, Fayoum University, Fayoum, 63514, Egypt

[3]Program in Developmental Biology, Institute of Biotechnology, University of Helsinki, Helsinki, Finland.

Correspondence

Eraqi R. Khannoon, Biology Department, College of Science, TaibahUniversity, Al-Madinah Al-Munawwarah, 344, Saudi Arabia. T:+966148618888-4327; E: err00@fayoum.edu.eg; ekhannoon@taibahu.edu.sa

Keywords

Viperinae: asynchronization; asymmetry; laterosphenoid; supraoccipital

Abstract

Ontogenetic studies are crucial for understanding functional morphology, origin and adaptation of skulls in vertebrates. However, very few studies have so far released complete embryonic series focusing on skull embryonic development in species showing diverse and extreme cranial morphologies such as snakes. The wide distribution and unique reproductive and ecological behaviors of venomous vipers, including the heterogeneity in breeding and egg incubation periods in oviparous species, make this group an excellent new model for studying the diversity of skull developmental processes in snakes. Here we present the first complete description of osteocranium development in a viperine snake, *Cerastes cerastes,* using detailed analysis of the ossification pattern of individual bones across different embryonic stages based on high-resolution microcomputed tomography data. Particularly, we describe in details the development of the laterosphenoid from its dorsal and ventral components, dividing the trigeminal foramen into maxillary and mandibular foramina. Furthermore, our data help clarifying some controversy concerning the presence and/or origin of structures related to the snake basicranium and braincase roof. For example, our detailed description of supraoccipital development suggests that this bone derived, at least in part, from the tectum posterius, although the involvement of the tectum synoticum cannot be totally excluded. Similarly, the epiotic centers of supraoccipital ossification are confirmed during braincase development, and the ancestral lacrimal bone primordium is observed as a ventral element at the early stages of prefrontal development. Finally, our embryonic *Cerastes cerastes* data highlight a plausible asymmetry in snake skull development, mostly occurring in the basicranium region, but further investigations of embryonic samples and viper species would be required to confirm such phenomenon.

Introduction

The research interest in squamate species (snakes and lizards) has rapidly increased in the recent years because of the key importance of this model in understanding fundamental questions about vertebrate evolution and development (Chang et al., 2009; Tzika et al., 2011; Sanger, 2012; Nomura et al., 2013; Diaz et al., 2017; Salomies et al., 2019; Macrì et al., 2019). Particularly, the observed variation in cranial structure, ossification and organization is remarkable within the whole of Squamata but also within specific clades of lizards and snakes, and appears tightly linked to both phylogenetic information and functional demands (Da Silva et al. 2018; Ollonen et al. 2018). Comparative analyses of skull bone development in squamates thus offer a unique opportunity to elucidate the developmental patterns and evolutionary origins of morphological diversity within amniotes, particularly extreme morphologies found in snakes. For this purpose, embryonic studies

are absolutely needed to describe the timing of morphogenesis and ossification of individual skull bones in a specific taxon, which can be then directly used for the comparison of developmental events across species. So far, despite the numerous anatomical descriptions of adult skull bones in many different snake species (see review; Cundall and Irish, 2008), investigations of craniofacial development and morphology in complete snake embryonic series, from oviposition to hatching, are still relatively rare (Boughner et al., 2007; Boback et al., 2012; Polachowsky and Werneburg, 2013; Khannoon and Evans, 2015; Sheverdyukova, 2017; Al Mohammadi et al., 2019; Sheverdyukova, 2019). Major challenges in previous studies have been the difficulty in getting a representative panel of snake samples covering the complete embryonic period of skull development (Bellairs and Kamal, 1981; Kamal and Hammouda, 1965a; Kamal and Hammouda, 1965b) and the dependence on histological stainings of serial head sections for description (Hofstadler-Deiques, 2002; Hofstadler-Deiques et al., 2005). Furthermore, the different methods used for embryonic skull visualization and description, including anatomical observations, several histological stains, alcian blue and alizarin red double-staining for cartilage and bone, and micro-computed tomography (CT) have caused variations in bone detection, morphology and developmental patterns. Especially, many important developmental and evolutionary questions remain to be answered using comparative, high-resolution assessment of structures related to the snake basicranium and braincase roof. For example, controversies exist regarding the laterosphenoid bone, particularly in the relative size of its dorsal and ventral components but also its formation by intramembranous ossification (Bellairs and Kamal, 1981). Similarly, the origin of the supraoccipital bone is highly debated, including in very recent studies (Khannoon and Evan, 2015; Al Mohammadi et al., 2019).

The Sahara horned viper (*Cerastes cerastes* Linnaeus, 1758) is a common venomous snake from Viperidae family widely distributed in Middle Eastern and North African deserts including Egypt (Baha El Din, 2006; The Reptile Database, accessed December 2019). *Cerastes* are relatively small, tapered, relatively thick-bodied snakes with a short tail averaging less than 50 cm in total length. They are nocturnal, terrestrial species capable of hiding in the sand by using their keeled, angled and serrated lateral scales in a rocking motion. Furthermore, they exhibit a unique sidewinding locomotion mode on both soft sand and hard surfaces. Similarly to other vipers, *Cerastes cerastes* shows a pair of relatively long solenoglyphous fangs that are used to inject venom from glands located towards the rear of the upper jaws (Johnson, 1958; Marx and Rabb, 1972). Each of the two fang is located on a relatively short and rotating maxillary bone that allows folding against the roof of the mouth when the jaws are closed. Other unique skull features of *Cerastes* genus include a bony snout relatively weakly attached to the braincase, long medial processes on the prefrontal bones, and a different arrangement and/or form of ectopterygoid and angular bones (El-Toubi and Magid, 1961). As an oviparous species, *Cerastes cerastes* offspring development

occurs outside of the mother's body, but oviposition happens usually later (around late July-early August) than other snakes inhabiting similar desert areas. Environmental conditions play a significant role in determining the breeding season of many reptiles (Schleich et al., 1996), and as other reptiles in desert areas, *Cerastes cerastes* snakes have a short breeding season. The time required for egg hatching is very different in viper species, reaching up to four months in pyramids viper (Al-Shammari, 2007), and the clutch size is about 9-16 eggs in *Cerastes cerastes*. Although a considerable number of studies have been conducted on reproductive aspects of reptiles from North African deserts and other similar environments, relatively little is known about skull development in Viperinae. Particularly, besides the analysis of both chondrocranium in *Cerastes vipera* (Kamal and Hammouda, 1965a) and osteocranium in a limited series of *Vipera aspis* embryos (two embryonic stages; Peyer, 1912), no complete skull development descriptions are available for this subfamily of venomous vipers. The unique skull morphology and ecological behaviors of the viperid *Cerastes,* but also the observed relatively short post-ovipositional embryonic period, make this snake a suitable new model for studying and expanding the diversity of skull developmental processes in snakes. Herein, we provide a complete morphological analysis of the post-ovipositional osteocranium development in the viperid *Cerastes cerastes*, by describing the ossification pattern of individual bones across different embryonic stages based on high-resolution CT scan data. The main purpose of this study was to expand our understanding of osteocranium development in viperids in order to help resolve a number of controversial issues related to the presence, origin and/or mode of development of skull elements from the snake basicranium and braincase roof, including the supraoccipital, laterosphenoid and prefrontal bones.

Materials and Methods

Samples

Female individuals of *Cerastes cerastes* were collected from the wild in Marsa Matruh, Egypt, and kept under field conditions in cages of 75 × 50 × 50 cm (L×W×H) with night/day temperature ranging from 27 to 32 °C. Animals were fed with mice until oviposition. Following oviposition at the end of July, fertilized eggs (N = 27) were collected and incubated at 30 ± 1 °C in plastic boxed filled with perlite at 90% moisture. The time from oviposition to hatchling at this temperature was 36 days post-oviposition (dpo; unpublished data). During early embryonic development, eggs were collected and opened every day. During the second half of embryonic development, eggs were opened every other days. Freshly extracted embryos were kept in phosphate buffered saline (PBS) for initial examination, before fixation in 4% paraformaldehyde (PFA) for at least 24 hours. Embryos were then washed in PBS and dehydrated in ascending ethanol series up to 100% Ethyl

alcohol, before micro-CT scanning. Staging of embryos was performed based on external characters using the complete developmental staging table available for Viperidae and Natricidae (Zehr, 1962; Tokita and Watanabe, 2019). To visualize osteocranium development, embryos were micro-CT scanned at different embryonic stages starting from stage 30 when the first ossification pattern could be recorded: stage 30 (8 dpo), stage 32 (12 dpo), stage 33 (15 dpo), stage 34 (19 dpo), early-stage 35 (22 dpo), mid-stage 35 (24 dpo), late-stage 35 (26 dpo), early-stage 36 (28 dpo), late-stage 36 (32 dpo) and stage 37 (35 dpo). A total of 27 and 18 embryos were used for staging and micro-CT scanning, respectively, corresponding to 1-3 embryos per developmental stage. All animal works and experiments were approved by the Zoology Department, Fayoum University, Faculty of Science on the Ethics of Animal Experiments.

Micro-CT scanning and 3D rendering

High-resolution micro-CT scans of embryonic skulls were produced at the Kumpula MicroCT facility of the University of Helsinki using Skyscan 1272 microCT with following parameters: filter: Al 0.25 mm; voltage: 60 kV; current: 166 µA; resolution: 13.207485 µm (stages 30-32), 11.000028 µm (stage 33, early-stage 36), 12.000013 µm (other stages). Samples were scanned in plastic immersed in 100 % ethanol. Scans were reconstructed using Bruker NRecon 1.1.17 software and the output files were assigned as .tiff images. 3D isosurface rendering from the reconstructed files as well as segmentation of cranial bones were done using the software Amira 5.5.0 (Thermo Fischer Scientific, U.S.A.). All 3D data were scaled by voxel size based on scan log file in Amira 5.5.0. Segmentation was done with the segmentation editor of Amira 5.5.0 based on image grey scale value thresholds, and surface files were created for skull bone visualization. Bone labeling was done using CorelDraw 2017 19.0.0.328 (Corel Corporation).

Results

Ossification Pattern of Skull Bones During Embryogenesis

We performed a detailed study of the ossification pattern and sequence in *Cerastes cerastes*, from onset of ossification to hatchling (Figs 1-7). This was done using high-resolution micro-CT data of developing skulls corresponding to 8 different embryonic stages between stage 30 (8 dpo) and stage 37 (35 dpo). Our descriptions follow the terminology and major skull regions previously defined for squamates (Cundall and Irish, 2008; McDowell 2008, Rieppel 1993). The bone that connects the quadrate to the rest of the skull in snakes is controversial in terms of homology and has been named either squamosal or supratemporal, depending on the author. Squamosal is the less commonly used term to represent this skeletal element, though the posterior placement of this bone articulates with

the posterior dorsomedial aspect of the quadrate as recorded for supratemporal in lizards (Cundall and Irish, 2008; Diaz and Trainor, 2019). For the sake of clarity and readability, it will be referred here as supratemporal, but we admit that it could be either of the previously mentioned bones when compared to lizards. We first provide general observations on the embryonic development of all skull bones (Figs 1-3), and the initial descriptive part for all individual bones generally refers to general features observed at stage 37 (Fig. 3, stage 37). Furthermore, we give a more detailed analysis on the origin and mode of development of controversial bones such as prefrontal (Fig. 4), supraoccipital (Fig. 5) and laterosphenoid (Figs 6 and 7).

Nasal

The nasal is a curved, irregularly shaped paired bone that covers nasal cavities dorsally at stage 37 (Fig. 3, stage 37). It contacts the septomaxillary and the frontal dorsally and antero-ventrally, respectively. Ossification is first visible at stage 32 (Fig. 1) as a curved triangular aggregation above the vomer. At stage 33, the bone expands ventrally and antero-laterally, becoming reminiscent of the final shape observed at stage 37 (Figs 1 and 3). The growth further continues at subsequent stages to reach the septomaxilla and the antero-ventral border of the frontal at stage 34 (Fig. 1) and mid-stage 35 (Fig. 2), respectively. The antero-lateral parts of the bone continue to expand towards the septomaxilla up to stage 37 (Fig. 3).

Parietal

The parietal bones are fused into one bone that forms a dome around the braincase by covering it dorsally. The descending process of parietal bones further covers the brain laterally in anterior postorbital parts, also forming the posterior part of the orbit, and contacts the postorbital medially, the sphenoid dorsally, and the prootic anteriorly. The dorsal part of the bone borders on the frontal postero-dorsally and contacts the prootic dorsally and the supraoccipital anteriorly. The descending processes of parietal bone ossify first starting from stage 30 (Fig. 1) as two convex, rectangular ossifications with a flat posterior edge, along with lateral margins of the dorsal part of parietal that extend posteriorly. The ossification is located postero-medially to the postorbital and anteriorly to the supratemporal. At stages 32 and 33, the bones grow ventrally towards the sphenoid but also dorsally, especially through a postero-dorsal projection extending posteriorly and connecting the postorbital (Fig. 1). At stage 34, lateral margins of the dorsal part of the bone expand medially in general, anteriorly towards the frontal, and dorsally towards the supraoccipital. Furthermore, the antero-ventral part of the descending process of parietal now connects the sphenoid (Fig. 1). At early-stage 35 (Fig. 2), both the anterior and posterior parts of the dorsal parietal expand in medial direction to border on the frontal as well as the prootic and supraoccipital. At this stage, the

descending process of the parietal also expands the close border with the sphenoid posteriorly. Between mid-stage 35 and early-stage 36, the anterior and posterior tips of the dorsal parietal continue to grow from opposing bones towards each other, with the presence of a minor medial expansion of ossification between them (Fig. 2). In addition, the ventral border of the descending process of parietal continues to expand posteriorly. At late-stage 36, the two separate parietal bones fuse at the anterior and posterior tips of the dorsal parietal, and a major medial ossification still happens throughout the bone (Fig. 3). The border between the sphenoid and the descending process of the parietal corresponds to the final skull at stage 37, and the bone already contacts the sphenoid, the prootic and the supraoccipital (Fig. 3). At stage 37, the bone is almost fully ossified apart from few unossified patches dorso-medially.

Premaxilla

At stage 37, the premaxilla is a slender, irregularly shaped unpaired bone that lacks teeth, apart from the caruncle (Fig. 3). It has a robust median dorsal process extending towards nasal bones as well as a flat, wide vomerine process that borders on both the septomaxilla and vomers antero-ventrally. The transverse processes are flat and rectangular structures extending towards the maxillae. The caruncle is visible as a hook-shaped and slender bone, which appears first antero-ventrally to the septomaxilla and vomers. At stage 30, this bone shows medial and transversal processes resembling adult shapes as well as two slender beginnings of a vomerine process along the bone tip (Fig. 1). At stage 32, the vomerine process expands posteriorly along with the premaxilla bone that establishes contact with the septomaxilla at stage 33 and the vomer at stage 34 (Fig. 1). The bone reaches its final shape at early-stage 35 (Fig. 2).

Maxilla

At stage 37, the maxilla is an irregularly shaped paired bone with a robust dentigerous surface bordering on the ectopterygoid and a flattened antero-dorsal part connecting the prefrontal antero-ventrally (Fig. 3). The dentigerous surface shows one erupted fang and 6 replacing fangs at different developmental stages. The bone first appears at stage 30 as a flat ossification with dorsally curved anterior tip posterior to the septomaxilla, lateral to the palatine and anterior to the ectopterygoid (Fig. 1). At stage 33, the bone already resembles its final shape and establishes contacts with the prefrontal bone, similarly to the situation at later stages (Fig. 1). The bone continues to grow from stage 34 (Fig. 1) to late-stage 36 (Fig. 3), and contacts with fangs and the ectopterygoid appear at early-stage 35 and late-stage 36, respectively (Figs 2 and 3). The first fang is completely ossified and connects the bone at stage 37 (Fig. 3).

Prefrontal

At stage 37, the prefrontal is an irregularly shaped, paired bone that forms a cavity anteriorly to the orbit (Fig. 3). The lacrimal foramen forms the anterior extremity of the cavity that expands and widens posteriorly. The prefrontal exhibits a long dorsal process at the anterior end, extending medially to cover most of the antero-dorsal edge of the frontal, and a minor postero-medial process extending medially (Fig. 3). Furthermore, the bone forms a sturdy v-shaped joint with the frontal antero-laterally and borders on the maxillary dorso-medially as well as the palatine antero-dorsally. The prefrontal appears first at stage 30, dorsally to the maxillary and anteriorly to the frontal, as two separate ossification centers: one for the medially extending antero-dorsal process and one for the rest of the bone (Figs 1 and 4). At stage 32, these centers fuse and the prefrontal already resembles its shape from stage 37, with almost complete cavity and lacrimal foramen (Figs 1 and 3). The bone continues to grow between stage 33 and late-stage 36 (Figs 1-3), becoming even more similar to stage 37 and establishing contacts with the maxilla and the palatine at stage 33 and mid-stage 35, respectively (Figs 1 and 2). The joint between the prefrontal and the frontal slowly becomes more rigid up to stage 37 (Figs 1-3, from stage 33 to stage 37).

Frontal

The frontal is a concavely rectangular (from dorsal view) paired bone that covers the forebrain region and expands ventrally to form most of the medial and antero-medial edge of the orbit (Fig. 3). Additionally, the anterior part of the bone expands laterally to form a firm connection with the prefrontal. The bone borders on the parietal antero-dorsally and the nasal postero-ventrally. It also exhibits connection with the sphenoid dorsally (Fig. 3). The bone appears first at stage 30 as a quadrifurcate ossification in the anterior parts of the future bone, posteriorly to the prefrontal (Fig. 1). At stage 32, this initial ossification expands towards the prefrontal joint as well as ventrally towards the septomaxilla and the sphenoid (Fig. 1). Such growth then continues both ventrally and posteriorly, and a dorsal ossification now expands at stage 33. At stage 34, the frontal bones contact each other dorsally and border on nasals at mid-stage 35 (Figs 2 and 3). The frontal bones are connected ventrally at late-stage 35, a stage where the bone also contacts the sphenoid. The bones continue to expand posteriorly to reach their final shape at late-stage 36 (Fig. 3).

Postorbital

The postorbital is a crescent-shaped paired bone that forms on the postero-lateral edge of the orbit and connects the descending process of the parietal laterally (Fig. 3). It first appears at stage 30 as a tiny ossification anteriorly to the descending process of the parietal, and then expands dorsally and ventrally at stage 32 (Fig. 1). At stage 33, the postorbital connects the parietal and already

resembles the hatchling shape (Figs 1 and 3). The bone continues to ossify antero-ventrally and antero-dorsally up to stage 37, curving around the orbit and becoming more robust in the process (Fig. 3).

Supratemporal

The supratemporal is a slender and flat paired bone with a spatula-like morphology, which corresponds to the dorso-lateral border of the parietal in its dorsal shape (Fig. 3). Both anterior and posterior ends contact the prootic laterally and the quadrate postero-ventrally, respectively, resting on the supratemporal dorso-laterally (Fig. 3). The supratemporal appears first as a thin and curved continuum of ossifications at stage 30, posteriorly to the parietal and dorsally to the pterygoid (Fig. 1). At stage 32, the bone widens and becomes curved and flat in shape (Fig. 1). It continues to grow between stages 33 and 34, where it reaches both the shape and position of stage 37, contacting the prootic (Figs 1 and 3). At mid-stage 35 (Fig. 2), the bone contacts the supraoccipital. The final growth then mostly occurs posteriorly, and contact with the quadrate is established at stage 37 (Fig. 3).

Quadrate

The quadrate is a long, slender trifurcate paired bone that flattens in the dorsal half to form a crescent-shaped surface for articulation at the ventral end (Fig. 3). Below the midline, the bone shows an ossified cyst in line with the stalk of stapes. The anterior end contacts the supratemporal postero-laterally and articulates with the compound bone dorsally (Fig. 3). The bone first appears at stage 32 (Fig. 1) as a perichondral ossification located in the middle of the quadrate cartilage, dorsally to the posterior part of the compound bone. Between stage 33 and mid-stage 35, the ossification expands towards the ventral and dorsal ends of the bone, with the cyst forming at the same time at stage 33, and the ventral end at mid-stage 35 already resembles the final stage 37 shape (Figs 2 and 3). At late-stage 36, the ventral surface is fully ossified in contrast to the dorsal end that remains open, with no endochondral ossification even visible at stage 37 (Fig. 3).

Vomer

The vomer is a paired bone that resembles a hollow water droplet by its general shape, albeit with robust posterior processes medially and minor, spike-like curved processes ventrally (Fig. 3). The vomer covers the vomeronasal organ, apart from organ's antero-dorsal side, and has several fenestrae on its postero-dorsal surface that form the majority of the fenestra vomeronasalis externa. The anterior part of the bone contacts the septomaxilla postero-ventrally and borders on the premaxilla posteriorly as well as the frontal antero-ventrally. It first appears at stage 30, ventrally to

the septomaxilla and medially to the palatine, as curved and thin ossifications flanked by minor ossification centers ventrally and dorsally (Fig. 1). At stage 32, the bone adopts a cuplike shape beneath the septomaxilla that forms the ventral edge of the fenestra vomeronasalis externa (Fig. 1). At stage 33, in addition to posterior processes, the ossification expands on the dorsal part of the bone and contacts both the septomaxilla and premaxilla, thus resembling the shape and position of stage 37 (Figs 1 and 3). Ossification of the bone then continues to spread slowly laterally around the dorsal edge of the fenestra vomeronasalis externa up to stage 37 (Fig. 3).

Palatine

The palatine is a slender, trifurcated and paired tooth-bearing bone that exhibits both a triangular anterior dentigerous process and a more rounded pterygoid process. It is connected to the pterygoid antero-medially and to the maxilla ventrally (Fig. 3). The bone appears first at stage 30 as a flat and semi-curved ossification medial to the maxillary and anterior to the pterygoid (Fig. 1). At stage 32, the bone expands towards both the maxillary and pterygoid, and the two processes are well visible (Fig. 1). The bone then continues growing to establish contact with the pterygoid and the prefrontal at stages 34 and mid-stage 35, respectively (Figs 1 and 2). Although the first signs of tooth ossification are already visible at stage 34 (Fig. 1), the bone continues to grow up to stage 37, and contacts with teeth are only established at this hatchling stage (Figs 1-3).

Pterygoid

The pterygoid is a long, feather-shaped, horizontally lying tooth-bearing paired bone with a wide and flat posterior quadrate process (Fig. 3). It exhibits a joint with the ectopterygoid ventrally in the middle of the bone and connects the palatine posteriorly. The dentigerous surface extends throughout its ventral surface. The bone appears first at stage 30 and shows the general morphological features of stage 37 posteriorly to the palatine and ventrally to the ectopterygoid and parietal (Figs 1 and 3). The bone continues to grow between stages 32 and 34, resembling the final shape and position of stage 37 already from stage 33, and establishes contact with the ectopterygoid at stage 33 and the palatine at stage 34 (Fig. 1). The first signs of tooth ossification appear at stage 34, but teeth only make contact with the bone at stage 37 (Figs 1-3).

Ectopterygoid

The ectopterygoid is a flat, spatula-shaped paired bone showing both a wide, bifurcated anterolateral end that contacts the maxillary and a thinner postero-medial end that connects the pterygoid (Fig. 3). The bone already appears as a spatula-shaped ossification at stage 30 (Fig. 1),

resembling the shape of stage 37 (Fig. 1). The bone continues growing to establish contact with the pterygoid at stage 33 and the maxilla at late-stage 36 (Figs 1-3).

Septomaxilla

The septomaxilla is a paired triangular bone that covers the vomeronasal organ antero-dorsally, forming the antero-dorsal part of the fenestra vomeronasalis externa. It has long and curved dorso-lateral processes as well as posterior condyles that contact nasals postero-laterally. Furthermore, the bone is connected to nasals postero-ventrally and premaxilla borders postero-ventrally (Fig. 3). The first ossifying parts are the dorso-lateral processes and the dorso-medial parts of the bone that together form a curved structure at stage 30, medially to the maxilla and antero-dorsally to the vomer (Fig. 1). At stage 32, the antero-medial portion and postero-medial condyles of the bone expand towards the prefrontal and nasals, respectively, and the bone grows anteriorly through the ossifying dorso-lateral process (Fig. 1). The position and shape of the septomaxilla resemble the hatchling shape starting from stage 33, and the bone borders on the premaxilla at stage 33 and contacts the nasals at stage 34 (Fig. 1).

Sphenoid

The sphenoid is an unpaired triangular-shaped bone that forms the braincase floor together with the basioccipital (Fig. 3). The bone results from the fusion of both intramembranous parasphenoid and endochondral basisphenoid. The parasphenoid part forms a stern notch-like attachment with the frontal bones ventrally and postero-ventrally, and it holds a large foramen in its dorso-medial part. The basisphenoid part is firmly attached to the descending process of the parietal on both sides ventro-laterally, and it contacts the prootic from the same direction. It also borders on the basioccipital anteriorly. The bone appears first at stage 32 in two separate regions (Fig. 1). In the anterior part of the future bone, the anterior tip of the parasphenoidal part appears as a spearhead-like ossification postero-ventrally to the frontal and antero-medially to the palatine. At the same stage, lateral edges of the basisphenoid appear postero-laterally as minor, curved ossification centers around trabeculae, located ventro-medially to the parietal and dorso-medially to the pterygoid (Fig. 1). At stage 33, the parasphenoid expands anteriorly, forming a bifurcated posterior end towards the basisphenoid as well as dorsal, finlike extensions towards frontals (Fig. 1). The basisphenoid expands with a tube-like ossification pattern around trabeculae ventro-medially to parietals, and its ossification also occurs at the crista stellaris. At stage 34, the two bones join from lateral sides and the basisphenoid expands towards the basioccipital and other bones laterally, but the pituitary fenestra and basicranial fenestra are not fully covered by bone yet (Fig. 1). The ossification then continues between early-stage 35 and late-stage 36, with the bone establishing

contact with the frontal at late-stage 35 and the parietal at late-stage 36 (Figs 2 and 3). The fenestrae are totally covered at late-stage 36, and contacts with the basioccipital and the prootic are established at early-stage 36 (Figs 2 and 3).

Basioccipital

At stage 37, the basioccipital is an unpaired and posteriorly curved pentagonal bone (from ventral view) showing an anterior fissure in the midline (Fig. 3). It contacts the sphenoid posteriorly, the prootic postero-ventro-laterally and the otooccipital ventro-medially, forming the ventral most edge of the foramen magnum. The bone appears first at stage 32 as a pentagonal aggregation of ossification centers ventro-medially to the otooccipital and medially to the posterior quadrate process of pterygoid (Fig. 1). At stage 33, the ossification expands and the basioccipital resembles the adult form, reaching the future foramen magnum, albeit with a hollow center and an anterio-medial part leaving a triangular unossified space (Fig. 1). The ossification continues between stage 34 and early-stage 35, with the center fully ossifying at early-stage 35 and the anterior end ossifying medially in a heart-like shape. The bone continues to expand at later stages, contacting the otooccipital, prootic and sphenoid at early-stage 36 (Figs 2 and 3).

Otooccipital

The otooccipital is an irregularly-shaped paired bone that forms from both exoccipital and opisthotic components (Fig. 3). It forms most of the foramen magnum, apart from the extreme ventro-medial edge that derived from the basioccipital, as well as the whole posterior and more than half of dorsal and ventral edges of the fenestra vestibularis. At stage 37, the opposing otooccipital bones are not yet fused together medially and are not even connected. However, the otooccipital contacts the basioccipital ventro-laterally, the prootic posteriorly and the supraoccipital both postero-laterally and posteriorly at this stage (Fig. 3). The otooccipital appears first at stage 30, as the exoccipital part ossifies around occipital arches as a paddle-shaped hollow aggregation postero-dorso-medially to the posterior quadrate process of the pterygoid, around lateral edges of the future foramen magnum (Fig. 1). The ossification continues at the exoccipital part at stage 32, when the ossification expands and becomes anchor-shaped (from lateral view) with flat dorsal expansions projected medially (Fig. 1). The first signs of ossification of the opisthotic part appear at stage 33, with a minor ossification expanding towards ossifying stapes (Fig. 1). At stage 34, the bone ossifies dorsally and medially from the exoccipital part towards the midline and the supraoccipital (Fig. 1). Additionally, the auditory capsule ossifies significantly at this stage, and the final features of the otooccipital are recognizable (Figs 1 and 3). The ossification continues between early-stage 35 and late-stage 35 (Fig. 2), with the foramen magnum and edges of the fenestra vestibularis becoming

established at late-stage 35. The bone contacts all basioccipital, supraoccipital and prootic bones at early-stage 36 (Fig. 2).

Supraoccipital (Fig. 4)

The supraoccipital is an unpaired bone that exhibits a convex-concave shape (from dorsal view), expanding ventro-laterally around the inner ear within the braincase (Fig. 3). It covers the postero-dorsal part of the braincase and flanks the brain dorso-laterally. The bone is connected to the parietal posteriorly and to the supratemporal postero-medially, and it borders on the prootic dorso-medially and the otooccipital postero-dorso-medially (Fig. 3). In squamate species, two different scenarios have been proposed for development of this bone (de Beer, 1937; Bellairs and Kamal, 1981): development from the tectum synoticum only, or development from both tectum synoticum and tectum posterius. The supraoccipital appears first at stage 34, anteriorly to the otooccipital and medially to the supratemporal, as one central unpaired ossification center surrounded by one pair of lateral centers (Figs 1 and 5, stage 34). The paired centers form as ossifications of the medial tips of the tectum synoticum in terms of shape and position, whereas the unpaired center corresponds to a flat, pentagonal or heart-shaped medial part of the future bone appearing between these paired centers (Fig. 5, stage 34). At early-stage 35, the bone expands towards all directions, establishing contact with the parietal (Figs 2 and 5, early-stage 35). Ossification continues at stages 35 and 36, with the bone contacting the supratemporal at mid-stage 35 as well as the prootic and the otooccipital at early stage 36 (Fig 2 and 3). All general bone features are recognizable starting from late-stage 35 (Fig. 2), and the bone borders on the prootic and the otooccipital at early-stage 36 (Figs 2 and 5). The ossification continues and the bone appears to cover the possibly related tectum synoticum structure at stage 36, whereas the medial part retains a spongy surface until hatching (Figs 3 and 5, stages 36 and 37).

Prootic

The prootic is an irregularly shaped paired bone that forms the lateral part of the braincase as well as the anterior and anterior-most parts of dorsal and ventral edges of the fenestra vestibularis (Fig. 3). The prootic contacts the parietal posteriorly and postero-laterally, the supratemporal anteriorly and the sphenoid dorso-medially, bordering on the otooccipital anteriorly and the supraoccipital antero-laterally (Fig. 3). The prootic appears first at stage 32 as several tiny ossifications on the lateral edges of the future bone, postero-ventrally to the ascending process of the parietal and anteriorly to the otooccipital, especially around the borders of the prootic notch. The bone ossifies from both lateral and anterior sides at stage 33, almost circling the trigeminal fenestra (Fig. 1). Edges of the fenestra vestibularis are also visible at this stage. At stage 34, the bone ossifies from all

sides, contacting the supratemporal, and totally circles the fenestra trigeminalis (Fig. 2). Importantly, signs of left-right asymmetry also appear at stage 34, with bones close to the future laterosphenoid being usually more apparent on the right side (see below and Fig. 6). At early-stage 35, the bone ossifies even further and the contact with the parietal is established (Figs 2 and 6). Between mid-stage 35 and early-stage 36, the ossification continues and the prootic resembles the hatchling form at early-stage 36 (Fig. 2). Furthermore, the bone establishes contact with the sphenoid and borders on the otooccipital and supraoccipital at similar stage (Fig. 2, early-stage 36). The final bone features of the prootic are already recognizable (Figs 2 and 3).

Laterosphenoid

The laterosphenoid is a paired, curved structure on the lateral edges of the prootic bone, forming an arch (also known as alethinophidian bridge) with the membranous extension of the prootic (Fig. 3). This arch covers the middle part of the fenestra trigeminalis. The laterosphenoid can be considered as part of the prootic bone but this bone is treated here separately to better highlight its development. At stage 37, the alethinophidian bridge is completed asymmetrically, as the laterosphenoid is only fused with the membranous extension of the prootic on one side (see below as well as Figs 3 and Fig. 7, stage 37). The laterosphenoid appears first at stage 34 as two separate extensions on the ventral edges of the trigeminal fenestra, which form the base of the future bone (Fig. 6, stage 34). These extensions fuse together and grow dorsally at early-stage 35 (Fig. 6, early-stage 35). The laterosphenoid then develops in continuity with the ventral membranous extension of the prootic. At mid-stage 35, the membranous extension of the prootic starts to ossify ventrally towards the laterosphenoid to form the dorsal portion of the future alethinophidian bridge (Fig. 7, mid-stage 35). From this stage, the timing of alethinophidian bridge formation appears variable between individuals, especially when comparing the left and right sides of the skull, indicating some asymmetry in development. Particularly, the membranous extension of the prootic and the laterosphenoid are separated by a gap on the right side at both mid-stage 35 and late-stage 36, indicating that the alethinophidian bridge is not complete yet (Fig. 7). In contrast, both the laterosphenoid and the membranous extension of the prootic are connected on the left side at similar stages, indicating that the alethinophidian bridge forms asymmetrically (Fig. 7, mid-stage 35). Similarly, at later stages, one side shows the membranous extension of the prootic and the laterosphenoid as separate entities, with the alethinophidian bridge exhibiting a minor line-like gap in the center (Fig. 7, stage 37, left side). On the other side, the separate parts are already fused together and the alethinophidian bridge forms a full arch dividing the trigeminal foramen, thus further highlighting the presence of left-right asymmetry at hatchling stage (Fig. 7, stage 37, right side). As seen at stage 37, the dorsal and ventral elements fuse at mid-distance, thus giving two

equal dorsal and ventral components for the laterosphenoid (Fig. 7). Importantly, some left-right symmetry in both the shape and size of the membranous extension of the prootic and the laterosphenoid are also apparent between stages 35 and 37, in addition to observed variations in the extent of their ossification (Figs 6 and 7).

Stapes

The stapes is a paired bone with a wide footplate in the middle of the fenestra vestibularis. It also forms a short stalk towards the quadrate, resembling a mushroom in shape. The bone appears first as minor ossification centers around the footplate at stage 33, posteriorly to the prootic bone (Fig. 1). At stage 34, the footplate has almost connected ossification centers, and the stalk starts his expansion from the footplate towards the quadrate. The ossification continues at later stages, with the footplate becoming solid at early stage 36 and the stalk continuing ossifying towards the quadrate until stage 37 (Figs 2 and 3).

Dentary

The dentary is a laterally v-shaped, tooth-bearing, paired bone exhibiting an open Meckelian groove, a large mental foramen and a strong bifurcation at the posterior end (Fig. 3). It borders on the compound bone and the splenial at stage 37 (Fig. 3). The bone appears first at stage 30 as several separate ossification centers on the anterior end of the future bone, which connect at stage 32 (Fig. 1). The ossification continues between stages 32 and 33, with a bifurcation appearing at the posterior end, and the mental foramen is surrounded by the bone at stage 33 (Fig. 1). At stage 34, the dentary contacts the splenial and the general features of the bone are already recognizable, with tips of the teeth starting to ossify (Fig. 1). After early stage 35, the anterior parts ossify slowly and are similar to stage 37 shape, whereas the posterior parts expand towards the compound bone to make contact at late-stage 35 (Fig. 2). The posterior parts resemble stage 37 shape only at late-stage 36, when the first tooth makes contact with the bone (Fig. 3).

Compound bone

The compound bone is a long, slender and tube-like paired bone exhibiting a bifurcated anterior end, a flat and curved prearticular ridge, a curved articular surface with high anterior and posterior borders, and a long, robust retroarticular process (Fig. 3). The Meckelian fossa shows an oval shape and the anterior half opens inside the bone. The bone articulates with the quadrate and contacts the dentary using a hinge-like fashion. Furthermore, it is connected to both the angular and the splenial postero-laterally. The bone first appears at stage 30 as three separate ossification centers, posteriorly to the dentary and ventrally to the posterior quadrate process of the pterygoid (Fig. 1). During this

phase, edges of the Meckelian fossa are already surrounded by the lateral-most ossification of the bone. At stage 32, the different parts fuse together to form a tube-like structure, the prearticular ridge is recognizable, and the bone expands anteriorly with some indication on the ossification of the retroarticular process (Fig. 1). At stage 33, the bone ossifies anteriorly, becoming clearly bifurcated, and expands at the prearticular ridge. Additionally, the retroarticular starts to be recognizable, with medial parts already ossifying and forming a complete tube in the rest of the bone (Fig. 1). At stage 34, the ossification continues in the aforementioned parts, and borders of the articular surface start to ossify. At early-stage 35, both the articular surface and the posterior end of the retroarticular process show ossification, sealing the posterior end of the bone (Fig. 2). At mid-stage 35, the bone resembles its final stage 37 shape from its posterior end, and it continues to expand anteriorly up to hatching, bordering on the dentary at early-stage 36 (Figs 2 and 3).

Splenial

The splenial is a small, trifurcated paired bone connected to the angular anteriorly, to the compound bone antero-medially and to the dentary postero-medially (Fig. 3). It appears first at stage 32 as a hockey stick-like ossification, medially to the posterior part of dentary (Fig. 1). At stage 33, the general shape of the bone is already recognizable and the bone establishes contact with the dentary (Fig. 1). From this stage, the bone continues to ossify slowly and establishes connection with the angular and the compound bone at late-stage 36 (Figs 2 and 3).

Angular

The angular is a small, rectangular paired bone that contacts the splenial posteriorly and the compound bone antero-medially (Fig. 3). The bone appears first at stage 32 as a tiny ossification medially to the anterior compound bone and postero-dorsally to the angular (Fig. 1). It ossifies relatively slowly, resembling stage 37 shape at stage 33 (Fig. 1). It establishes contact with the compound bone at mid-stage 35 (Fig. 2) and the splenial at late-stage 36 (Fig. 3).

Discussion

We present here one of the very few descriptions of the embryonic development of the osteocranium in the Viperinae subfamily of venomous vipers. Previous analyses of viper skull development have mostly focused on the Crotalinae subfamily, with descriptions published for species such as *Agkistrodon piscivorus* and *Bothropoides jararaca* (reviewed in Ollonen et al, 2018). To our knowledge, only one incomplete description of osteocranium development in *Vipera aspis* (two embryonic stages; Peyer 1912) is currently available for Viperinae.

Comparison of snake oviposition period and osteogenesis

The time required for egg hatching is very different among oviparous snakes, ranging from a few weeks to up to four months in viper species. It is worth noting that variations in the timing of egg incubation and hatchling could also be reflected by different incubation temperatures. We describe here that *Cerastes cerastes* snakes show a period of post-ovipositional development of 36 dpo at a temperature of 30±1°C, which is relatively short when compared to our previous descriptions of snakes from Egypt such as *Naja haje* (51-54 dpo, Khannoon and Evans, 2014, 2015) and *Psammophis sibilans* (49-50 dpo, Khannoon and Zhardanicek, 2016). We assume that this short oviposition period could be linked to an extended retainment of eggs prior to oviposition, thus resulting in a latency in oviposition, and/or a global acceleration in embryonic development, which is reflected by the relatively late embryonic stage of this species at oviposition (personal observations). Similarly to other squamates analyzed, bones of the dermatocranium are among the first to ossify in *Cerastes cerastes* (Tables 1 and 2). However, at stage 30, corresponding to less than a quarter of the total post-ovipositional period (8 dpo), more than half of the bones analyzed such as premaxilla, maxilla, prefrontal, supratemporal, palatine, pterygoid, ectopterygoid, septomaxilla, dentary and compound bone have already started to ossify in *Cerastes cerastes* (Table 1). By contrast, the ossification pattern of the above mentioned bones is more gradual in P*sammophis sibilans*, starting first in supratemporal, palatine and compound bone (Table 2, rank 1), then in pterygoid, premaxilla, maxilla, prefrontal, ectopterygoid and dentary (ranks 2 and 3), and finally in septomaxilla (rank 5; Al Mohammadi et al., 2019). In *Naja haje*, ossification of these bones also starts at different developmental stages (Table 2; Khannoon and Evans, 2015), occurring more gradually than in *Cerastes cerastes*. Importantly, other bones appearing later in all species generally follow the same pattern where they develop earlier in *Cerastes cerastes* than in other oviparous species (Table 2; Haluska and Alberch, 1983; Jackson, 2002 ; Boughner et al., 2007; Polachowsky and Werneburg, 2013; Sheverdyukova, 2017; Sheverdyukova, 2019). One exception to this pattern is the early development of some bones such as premaxilla, palatine, pterygoid, ectopterygoid, dentary, and articular in *Naja kaouthia* (Table 2; Jackson, 2002).

Origin of supraoccipital

Our results on the osteocranium of *Cerastes cerastes* show that the supraoccipital bone develops first at stage 34 as separate unpaired and paired ossification centers anteriorly to the otooccipital. The paired centers are located antero-medially to the auditory capsule and postero-laterally adjacent to the calcified endolymphatic sacs, a position that can be referred as epiotic. Indeed, this position is similar to previous descriptions of epiotic ossification in snakes (Parker,

1879; Khannoon and Evans, 2015; Sheverdyukova, 2017), also confirming the presence of epiotic centers of ossification. At the same stage, a pentagonal unpaired ossification appears in a medial, separate position from the epiotic ossified center. The latter could correspond to ossification of the intercapsular cartilage, named as intercapsular plate by Khannoon and Evans (2015), which showed a similar heart-like shape. In favor of that, the supraoccipital is known as an endochondral bone developing from cartilaginous precursors. However, the limitation of micro-CT scans in not showing cartilage structures cannot resolve the exact source cells of supraoccipital ossifications. Other techniques such as histology and/or lineage tracing of such cartilaginous cells would be needed to identify the exact precursors of supraoccipital in snakes. Particularly, the visualization and identification of the cartilaginous component as tectum synoticum only (capsular origin) (De Beer, 1937; Kamal, 1981), tectum posterius only (occipital arches origin) (Khannoon an Evans, 2015) or both (Al Mohammadi et al., 2019) would be needed to help clarifying the debate on supraoccipital origin. Based on the current study, despite the absence of detection of cartilaginous elements in micro-CT scans, our data indicate that the only explanation for the observed ossification pattern is an endochondral ossification extending from the epiotic centers medially and posteriorly, contacting the extending ossification of the intercapsular cartilage (described here as the medial part) that extends in opposite directions. Furthermore, a relatively similar ossification pattern for supraoccipital development has been already described in the elapid snake *Naja haje* (Khannoon and Evans, 2015), rather suggesting a tectum posterius origin for the supraoccipital, which originates from occipital arches. However, other hypotheses cannot be excluded based on our findings, thus increasing the controversy related to supraoccipital origin. Particularly, we disagree with the reports of Bellairs and Kamal (1981) and De Beer (1937), suggesting that the supraoccipital is completely of tectum synoticum origin (derived from the capsular material) because of the lack of tectum posterius in snakes. Indeed, for now an elapid *Naja haje*, a colubrid *Psammophis sibilans*, and possibly the current studied viperid *C. cerastes* showed different scenarios of development, with a full or partial origin from occipital arches. Such disparity could be likely explained by the few stages that have been considered so far in previous tectum studies for snakes. On the other hand, the way the intercapsular tectum develops is a point of variation between snakes (El Toubi and Kamal, 1965). The epiotic centers constitute another point of controversy, because although their presence have been confirmed by Parker (1879), Khannoon and Evans (2015), Sheverdyukova (2017) and this study, other scientists have doubted their presence (De Beer, 1937; Bellairs and Kamal, 1981; Al Mohammadi et al., 2019), suggesting that some variation might also exist between snake species regarding ossification centers. Altogether, it seems mandatory not to depend on only one technique for fully undesrtanding the development of the braincase roof in snakes, and complementary, comparative approaches should be used.

Formation of laterosphenoid

Our data indicate disparity regarding laterosphenoid development in snakes. Bellairs and Kamal (1981) suggested the ventral part to form most of the laterosphenoid. Our observations in *Cerastes cerastes* rather indicate that the dorsal and ventral elements of laterosphenoid meet each other almost in the midway, whereas the dorsal element was twice the length of the ventral element in *Psammophis sibilans* (Al Mohammadi et al., 2019). These observations suggest the existence of interspecific variation in the extent of contribution of dorsal and ventral elements to laterosphenoid formation in snakes. The laterosphenoid is a fully intramembranous bone (Bellairs and Kamal, 1981; Al-Mohammadi et al., 2019), and our results clearly show a gradual development of this bone from its dorsal and ventral elements. The ventral element develops first as two separate extensions on the ventral edges of the trigeminal foramen, which form the base of the future bone. In accordance with Al-Mohammadi et al (2019), we further show that the dorsal element originates from the lateral side of the prootic at the position of the anterior semicircular canal. Final development of the laterosphenoid with formation of the alethinophidian bridge divides the trigeminal foramen into mandibular and maxillary foramina. Additionally, we highlight possible left/right asymmetry in the ossification pattern of the *Cerastes cerastes* laterosphenoid between mid-stage 35 and stage 37. Although very interesting, these observations would require further validation using an increased number of embryonic samples as, to our knowledge, such phenotype has rarely been reported in common squamate reptiles. Indeed, asymmetric jaws have been already described at least in snail-eating terrestrial snakes (family Pareida; Hoso, 2017), a phenotype associated with dietary specialization, but cranial asymmetry has been rather shown to be a convergent trait widely distributed across animals colonizing extreme environment such as cavefish (Powers et al., 2017) and fossorial uropeltid snakes (Olori and Bell, 2012).

Two prefrontal ossification centers give indication of lacrimal bone

The presence of lacrimal bone is ancestral in squamates, existing in most lizards (Evans, 2008), but it has not been recorded in any living or extinct snake so far (Rieppel et al., 2003; Zaher and Rieppel, 2012). However, the multiple ossification centers previously identified in snakes could be of interest considering the ventral center as a primordium of the lacrimal bone (Boughner et al., 2007; Khannoon and Evans, 2015; Sheverdyukova, 2017). The ventral center is exactly at the position where the lacrimal bone would develop, and where it definitely lies in lizards. Furthermore, the prefrontal was recently shown to be a cryptic bone (Diaz and Trainor, 2019), with the ventral component also identified as the lacrimal and the dorsal component a ventrally expanding prefrontal bone. In *Cerastes cerastes*, two different centers of ossification for the prefrontal were identified at stage 30, including a slenderer ventral center. A similar pattern of ossification has been previously

observed in different snake species from different families, including *Naja haje* (Khannoon and Evans, 2015), *Natrix natrix* (Sheverdyukova, 2019) and *Psammophis sibilans* (Al Mohammadi et al., 2019), further suggesting that the ventral center might correspond to the position of the lacrimal primordium. Importantly, the use of micro-CT in our studies enabled us to visualize the ossification centers precisely from different angles, thus confirming their number and separation, in contrast to previous analyses using skeleton staining or even histology.

Conclusions

Our detailed description of osteocranium development in the viperine snake *Cerastes cerastes* showed similarities with other snakes, but some interesting differences were also noticed, including in the bone ossification pattern. Although the fate of cartilaginous components of the skull could not be detected using micro-CT, this advanced technique was useful to identify new details not detected in previous snake studies, even those using complete series of embryos (Boughner et al., 2007; Boback et al., 2012; Khannoon and Evans, 2015, Al Mohammadi et al., 2019). Particularly, it enabled us to accurately follow basicranium development, including the dorsal and ventral components of laterosphenoid and the time they eventually fuse and divide the trigeminal foramen. Similarly, our data suggest that the supraoccipital derived, at least in part, from the tectum posterius, so the contention related to supraoccipital development might be attributed to different developmental behaviors and/or different snake species. Our results also confirm the presence of ancestral structures in snakes, which is here shown by the lacrimal primordium. Finally, the observed asymmetry in the basicranium region during skull development suggests that this phenomenon might occur in at least some snake species. Future studies including more samples and snake species may confirm this interesting finding.

Acknowledgements

Our Thanks go to Hagar Ibrahim Bayoumi (Fayoum University) for help with sample collection and processing.

References

Al Mohammadi AGA, Khannoon ER, Evans SE (2019) The development of the osteocranium in the snake *Psammophis sibilans* (Serpentes: Lamprophiidae). *J Anat* **236**, 117–131.

Al-Shammari AM (2007) Ecological, ecophysiological and toxicological aspects of the pyramid viper, *Echis pyramidum* in Jazan province Department of Zoology, College of Science, King Saud University; Riyadh, Saudi Arabia. Ph.D. dissertation.

Baha El Din S (2006) *A Guide to the Reptiles and Amphibians of Egypt*, pp. 359. Cairo: AUC Press.

Bellairs Ad'A, Kamal AM (1981) The chondrocranium and development of the skull in recent reptiles. In: *Biology of the Reptilia*, Volume 11, Morphology F (eds Gans C, Parsons TS), pp. 1–263. Academic Press.

Boback SM, Dichter EK, Mistry HL (2012) A developmental staging series for the African house snake, *Boaedon* (*Lamprophis*) *fuliginosus*. *J Zool* **115**, 38–46.

Boughner JC, Buchtova M, Katherine Fu, et al. (2007) Embryonic development of *Python sebae* – I: staging criteria and macroscopicskeletal morphogenesis of the head and limbs. *J Zool* **110**, 212–230.

Chang C, Wu P, Baker RE, et al. (2009) Reptile scale paradigm: Evo-Devo, pattern formation and regeneration. *Int J Dev Biol* **53**, 813–826.

Cundall D, Irish F (2008) The snake skull. In: *Biology of the Reptilia*, Volume 20, Morphology H (eds Gans C, Gaunt AS, Adler K), pp. 349–692. New York: SSAR.

Da Silva FO, Fabre AC, Savriama Y, et al. (2018) The ecological origins of snakes as revealed by skull evolution. *Nat Commun* **9**, 376.

De Beer GR (1937) *The Development of the Vertebrate Skull*. Reprinted 1985 edition, pp. 554. Chicago: University of Chicago Press.

Diaz RE Jr, Bertocchini F, Trainor PA (2017) Lifting the veil on reptile embryology: the veiled chameleon (*Chamaleo calyptratus*) as a model system to study reptilian development. *Methods Mol Biol* **1650**, 269–284.

Diaz RE Jr, Trainor PA (2019) An integrative view of Lepidosaur cranial anatomy, development and diversification. In: *Heads, jaws and muscles anatomical, functional and developmental diversity in chordate evolution* (eds Ziermann J, Diaz Jr RE, Diogo R), pp. 207–227. Springer.

El Toubi MR, Kamal AEM (1965) The origin of the tectum of the occipitoauditory region in Squamata. *Proc Egypt Acad Sci* **18**, 73–75.

Evans SE (2008) The skull of lizards and tuatara. In: *Biology of the Reptilia*, Volume 20, Morphology H (eds Gans C, Gaunt AS, Adler K), pp. 1–347. New York: SSAR.

Haluska F, Alberch P (1983) The cranial development of *Elaphe obsoleta* (Ophidia, Colubridae). *J Morphol* **178**, 37–55.

Hofstadler-Deiques C (2002) The development of the pit organ of *Bothrops jararaca* and *Crotalus durissus terrificus* (Serpentes,Viperidae): support for the monophyly of the subfamily Crotalinae. *Acta Zool* **83**, 175–182.

Hofstadler-Deiques C, Walter M, Mierlo F, et al. (2005) Software system for three-dimensional volumetric reconstruction of histological sections: a case study for snake chondrocranium. *The Anat Rec* **286A**, 938–944.

Hoso M (2017) Asymmetry of mandibular dentition is associated with dietary specialization in snail-eating snakes. *PeerJ* **5**, e3011.

Jackson K (2002) Post-ovipositional development of the monocled cobra, *Naja kaouthia* (Serpentes: Elapidae). *Zool* **105**, 203–214.

Johnson BD, (1968) Selected Crotalidae venom properties as a source of taxonomic criteria. *Toxicon* **6**, 5–10.

Kamal AM, Hammouda HG (1965a) The development of the skull of *Psammophis sibilans*. II. The fully formed chondrocranium. *J Morphol* **116**, 247–296.

Kamal AM, Hammouda HG (1965b) The development of the skull of *Psammophis sibilans*. III. The osteocranium of a late embryo. *J Morphol* **116**, 297–310.

Khannoon ER, Evans SE (2014) The embryonic development of the Egyptian cobra *Naja haje* (Squamata: Serpentes: Elapidae). *Acta Zool* **95**, 472–483.

Khannoon ER, Evans SE (2015) The development of the skull of the Egyptian Cobra *Naja h. haje* (Squamata: Serpentes: Elapidae). *Plos One* **10**, e0122185.

Khannoon ER, Zahradnicek O (2017) Postovipositional development of the sand snake *Psammophis sibilans* (Serpentes: Lamprophiidae) in comparison with other snake species. *Acta Zool* **98**, 144–153.

Macrì S, Savriama Y, Khan I, et al. (2019) Comparative analysis of squamate brains unveils multi-level variation in cerebellar architecture associated with locomotor specialization. *Nat Commun* **10**, 5560.

Marx H, Rabb GB (1972) Phyletic analysis of fifty characters of advanced snake. *Fieldiana Zool* **63**, 1–321.

Nomura T, Kawaguchi M, Ono K, et al. (2013) Reptiles : a new model for brain evo-devo research. *J Exp Zool B Mol Dev Evol* **320**, 57–73.

Olori JC, Bell CJ (2012) Comparative skull morphology of uropeltid snakes (Alethinophidia: Uropeltidae) with special reference to disarticulated elements and variation. *PLos One* **7**, e32450.

Ollonen J, Da Silva FO, Mahlow K, et al. (2018) Skull development, ossification pattern, and adult shape in the emerging lizard model organism *Pogona vitticeps*: a comparative analysis with other squamates. *Front Physiol* **9**, 278.

Parker WK (1879) On the structure and development of the skull of the common snake (*Tropidonotus natrix*). *Philos Trans R Soc Lond* **169**, 385–417.

Peyerb (1912) Die Entwicklung des Schadelskelettes von *Viper aaspis. Morph Bot Jahrb Syst* **44**, 563–621.

Polachowski KM, Werneburg I (2013) Late embryos and bony skull development in *Bothropoides jararaca* (Serpentes, Viperidae). *J Zool* **116**, 36–63.

Powers AK, Davis EM, Kaplan SA, et al. (2017) Cranial asymmetry arises later in the life history of the blind Mexican cavefish, *Astyanax mexicanus*. *PLos One* **12**, e0177419.

Rieppel O, Zaher H, Tchernov E, et al. (2003) The anatomy and relationships of *Haasiophis terrasanctus*, a fossil snake with well-developed hind-limbs from the mid-Cretaceous of the Middle East. *J Paleontol* **77**, 536–558.

Salomies L, Eymann J, Khan I, et al. (2019) The alternative regenerative strategy of bearded dragon unveils the key processes underlying vertebrate tooth renewal. *Elife* **8**, e47702.

Sanger TJ (2012) The emergence of squamates as model systems for integrative biology. Evol Dev **14**, 231–233.

Schleich HH, Kästle W, Kabisch K (1996) *Amphibians and Reptiles of North Africa*, 627 pp. Koenigstein: Koeltz.

Sheverdyukova HV (2017) Development of the osteocranium in *Natrix natrix* (Serpentes, Colubridae) embryogenesis I: development of cranial base and cranial vault. *Zoomorphol* **136**, 131–143.

Sheverdyukova HV (2019) Development of the Osteocranium in *Natrix natrix* (Serpentes, Colubridae) Embryogenesis II: Development of the jaws, palatal complex and associated bones. *Acta Zoologica* **100**, 282–291.

Tokita M, Watanabe H (2019) Embryonic development of the Japanese mamushi, *Gloydius blomhoffii* (Squamata: Serpentes: Viperidae: Crotalinae). *Curr Herpetol* **38**, 6–13.

Tzika AC, Helaers R, Schramm G, et al. (2011) Reptilian-transcriptome v1.0, a glimpse in the brain transcriptome of five divergent Sauropsida lineages and the phylogenetic position of turtles. *Evodevo* **2**, 19.

Zaher H, Rieppel O (2012) The skull of the Upper Cretaceous snake *Dinilysia patagonica* Smith-Woodward, 1901, and its phylogenetic position revisited. *Zool J Linn Soc* **164**, 194–238.

Zehr DR (1962) Stages in the normal development of the common garter snake, *Thamnophis sirtalis sirtalis*. *Copeia* **1962**, 322–329.

Figure and table legends:

Figure 1: Embryonic development of skull bones in *Cerastes cerastes* at stage 30 (8 days post-oviposition or dpo), stage 32 (12 dpo), stage 33 (15 dpo) and stage 34 (19 dpo) in dorsal (left panels) and lateral (right panels) views. Abbreviations: Na = nasal, P = parietal, Prx = premaxilla, Mx = maxilla, Prf = prefrontal, F = frontal, Po = postorbital, St = supratemporal, Q = quadrate, Vo = vomer, Pal = palatine, Pt = pterygoid, Ec = ectopterygoid, Spx = septomaxilla, Sp = sphenoid, Bo = basioccipital, Oto = otooccipital, So = supraoccipital, Pro = prootic, Stp = stapes, D = dentary, Cb = compound bone, Spl = splenial, An = angular, CE = calcified endolymph, Stm = statolithic mass. Scale bars = 1 mm.

Figure 2: Embryonic development of skull bones in *Cerastes cerastes* at early-stage 35 (22 dpo), mid-stage 35 (24 dpo), late-stage 35 (26 dpo) and early-stage 36 (28 dpo) in dorsal (left panels) and lateral (right panels) views. For further details, see Figure 1.

Figure 3: Embryonic development of skull bones in *Cerastes cerastes* at late-stage 36 (32 dpo) and stage 37 (35 dpo) in dorsal (left panels) and lateral (right panels) views. For further details, see Figure 1.

Figure 4: Fronto-lateral view of *Cerastes cerastes* skull at stage 30 highlighting two segmented ossification centers of prefrontal bone (Prf, colored bone). Scale bar = 1 mm.

Figure 5: Embryonic development of the supraoccipital bone in *Cerastes cerastes* in occipital view between stage 34 and stage 37. The lateral paired and central unpaired ossification centers are segmented with different colors at stage 34, and the supraoccipital bone is further highlighted in purple color at subsequent stages. Abbreviations: Eo = Epiotic ossification, Io =Intercapsular ossification, Nao = neural arch origin. Scale bars = 1 mm.

Figure 6: Left (left panels) and right (right panels) lateral views of the ossification pattern of the prootic bone between stage 32 and early-stage 35. Initial formation of the laterosphenoid bone is segmented in pink color. Abbreviations: f5 = trigeminal foramen, f5b = foramen for maxillary

branch of trigeminal, f5c = foramen for mandibular branch of trigeminal, Ls = laterosphenoid, Mep = membranous extension of the prootic bone. Scale bars = 1 mm.

Figure 7: Left (left panels) and right (right panels) lateral views of the ossification pattern of the prootic bone between mid-stage 35 and stage 37. Both the ventral membranous extension of the prootic and the laterosphenoid bone are segmented in pink color. For further details, see Figure 6.

Table 1: Ossification sequence of individual skull bones from the dermatocranium, neurocranium and splanchocranium between stage 30 and stage 37 in *Cerastes cerastes*. Marks and grey shading indicate the presence of ossification based on micro-CT data.

Table 2: Comparison of the onset of bone ossification (in developmental stages (Stg), dpo and/or ranks) in various oviparous snake species with data available: *Cerastes cerastes* (this article)*, Naja kaouthia* (Jackson, 2002)*, Naja haje* (Khannoon and Evans, 2015)*, Python sebae* (Boughner et al., 2007), *Psammophis sibilans* (Al Mohammadi et al., 2019)*, Pantherophis alleghaniensis* (Haluska and Alberch, 1983), and *Natrix natrix* (Sheverdyukova, 2017; Sheverdyukova, 2019). The total post-ovipositional incubation period is also indicated for each species.

Table 1.

Dermatocranium:	Stage 30	Stage 32	Stage 33	Stage 34	Early-stage 35	Mid-stage 35	Early-stage 36	Late-stage 36	Stage 37
Nasal		X	X	X	X	X	X	X	X
Parietal	X	X	X	X	X	X	X	X	X
Premaxilla	X	X	X	X	X	X	X	X	X
Maxilla	X	X	X	X	X	X	X	X	X
Prefrontal	X	X	X	X	X	X	X	X	X
Frontal	X	X	X	X	X	X	X	X	X
Postorbital	X	X	X	X	X	X	X	X	X
Supratemporal	X	X	X	X	X	X	X	X	X
Vomer	X	X	X	X	X	X	X	X	X
Palatine	X	X	X	X	X	X	X	X	X
Pterygoid	X	X	X	X	X	X	X	X	X
Ectopterygoid	X	X	X	X	X	X	X	X	X
Septomaxilla	X	X	X	X	X	X	X	X	X
Dentary	X	X	X	X	X	X	X	X	X
Compound bone	X	X	X	X	X	X	X	X	X
Splenial		X	X	X	X	X	X	X	X
Angular		X	X	X	X	X	X	X	X

Neurocranium:	Stage 30	Stage 32	Stage 33	Stage 34	Early-stage 35	Mid-stage 35	Early-stage 36	Late-stage 36	Stage 37
Sphenoid	X	X	X	X	X	X	X	X	X
Basioccipital		X	X	X	X	X	X	X	X
Otooccipital	X	X	X	X	X	X	X	X	X
Supraoccipital				X	X	X	X	X	X
Prootic		X	X	X	X	X	X	X	X
Laterosphenoid				X	X	X	X	X	X

Splanchocranium:	Stage 30	Stage 32	Stage 33	Stage 34	Early-stage 35	Mid-stage 35	Early-stage 36	Late-stage 36	Stage 37
Quadrate		X	X	X	X	X	X	X	X
Stapes			X	X	X	X	X	X	X

Table 2.

	C. cerastes		*N. kaouthia*		*N. haje*		*P. sebae*		*P. sibilans*		*P. Allegha-niensis*		*N. natrix*	
Incubation period (dpo)	35		60-65		51-54		80-90		49-51		74-79		30-31	
Onset of ossification	Stg	Rank	Stg	Rank	Stg	Rank	Stg	Rank	Stg	Rank	dpo	Rank	Stg	Rank
Nasal	32	2	8	3	7a	3	4	2	late 7-8	6	36	3	32	3
Parietal	30	1	8	3	7a	3	6	3	5	1	36	3	31	2
Premaxillary	30	1	3	1	6b	2	6	3	6	3	24	1	31	2
Maxillary	30	1	<7	2	6a	1	4	2	6	3	36	3	32	3
Prefrontal	30	1	8	3	6a	1	4	2	6	3	36	3	31	2
Frontal	30	1	8	3	7a	3	6	3	7-8	5	36	3	31	2
Postorbital	30	1	8	3	7a	3	6	3	7-8	5	48	5	34	5
Supratemporal	30	1	<7	2	6a	1	4	2	5	1	36	3	31	2
Vomer	30	1	8	3	6b	2	6	3	7-8	5	36	3	31	2
Palatine	30	1	3	1	6a	1	4	2	5	1	24	1	30	1
Pterygoid	30	1	3	1	6a	1	3	1	23	2	24	1	30	1
Ectopterygoid	30	1	3	1	6a	1	6	3	6	3	24	1	31	2
Septomaxillary	30	1			7a	3	6	3	7-8	5	30	2	33	4
Dentary	30	1	3	1	6a	1	4	2	6	3	36	3	32	3
Compound bone	30	1	8	3	6a	1	4	2	5	1	30	2	31	2
Splenial	32	2	8	3	7a	3	4	2	7-8	5	36	3	32	3
Angular	32	2	8	3	7a	3	6	3	7-8	5	30	2	32	3
Parasphenoid	30	1	10	5	7a	3	7	4			52	7	33	4
Basisphenoid	30	1	8	3	7a	3	7	4	6	3	41	4	33	4
Basioccipital	32	2	8	3	6a	1	8	5	7-8	5	36	3	31	2
Otooccipital	30	1	8	3	6b	2	6	3	7	4	30	2	30	1
Supraoccipital	34	4	8	3	7a	3	6	3	late 7-8	6	59	8	34	5
Prootic	32	2	8	3	6a	1	7	4	6	3	49	6	33	4
Laterosphenoid	34	4	10?	5?	8	5	10?	6?	7-8	5	50	7		
Quadrate	32	2	8	3	6b	2	7	4	23	2	41	4	32	3
Articular	22	5	3	1	7a	3	6	3					36	6
Staped	33	3							late 7-8	6	59	75	34	5
Tooth on dentary	34	4	8	4	7b	4	10	5	late 7-8	6				
Tooth on Maxillary	22	5	8	4	7a	3	7	4	late 7-8	6				
Tooth on Palatine	34	4	10	5	8	5	10	5	late 7-8	6				

Stage 30 (8 dpo)

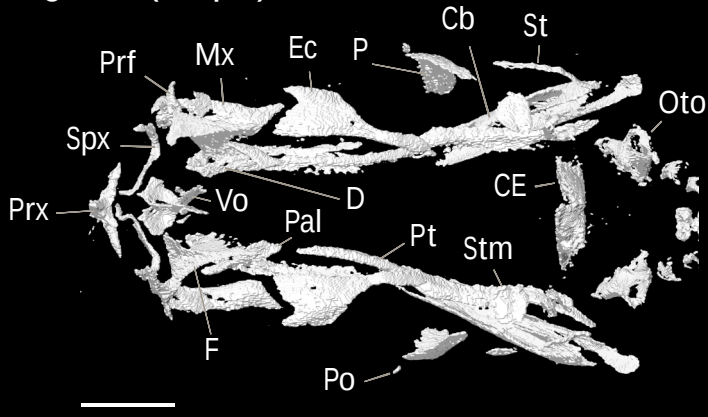

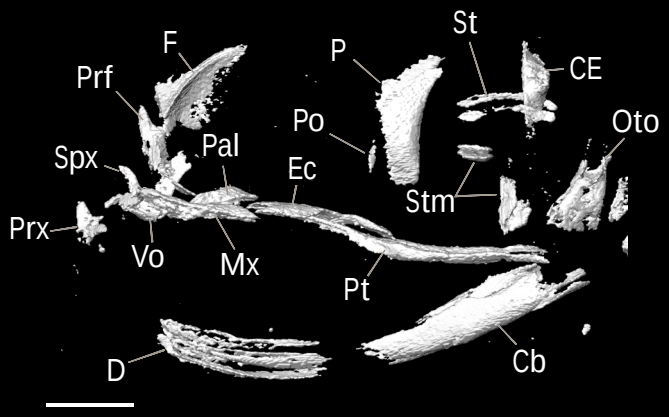

Stage 32 (12 dpo)

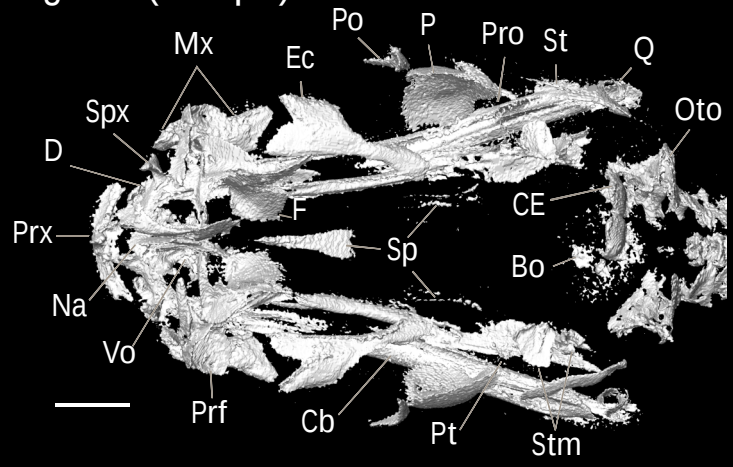

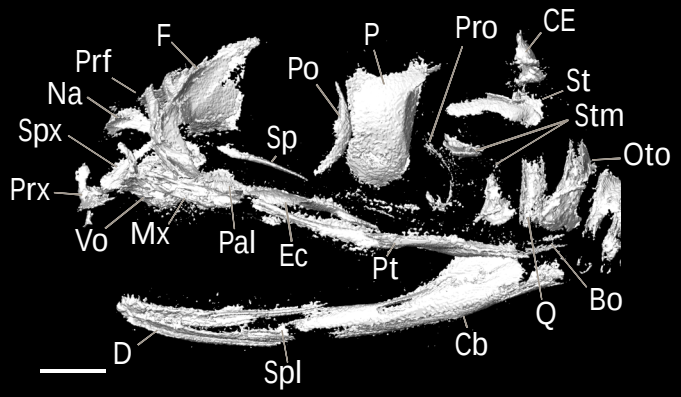

Stage 33 (15 dpo)

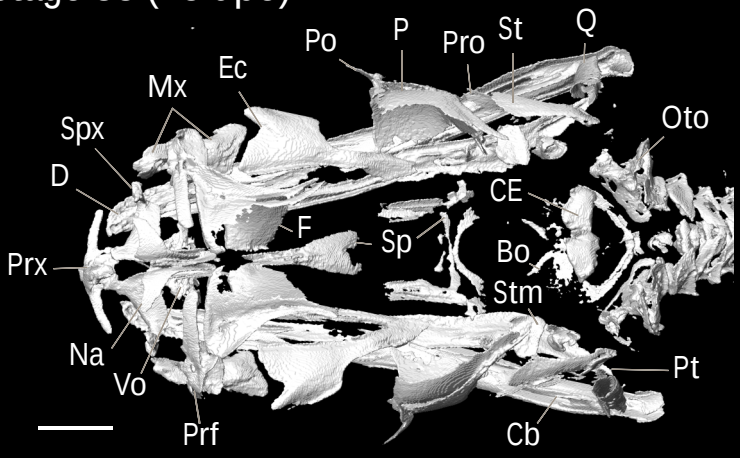

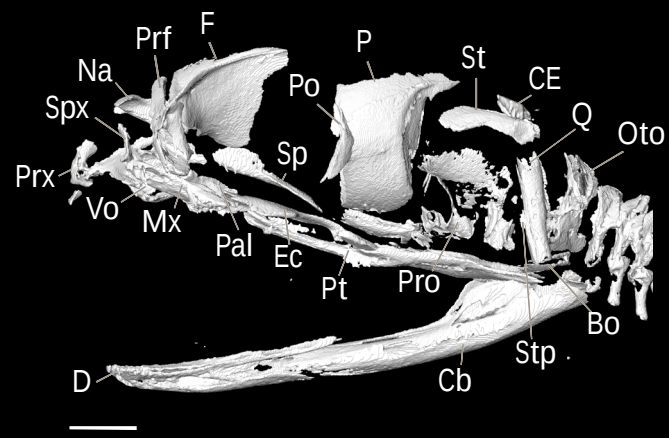

Stage 34 (19 dpo)

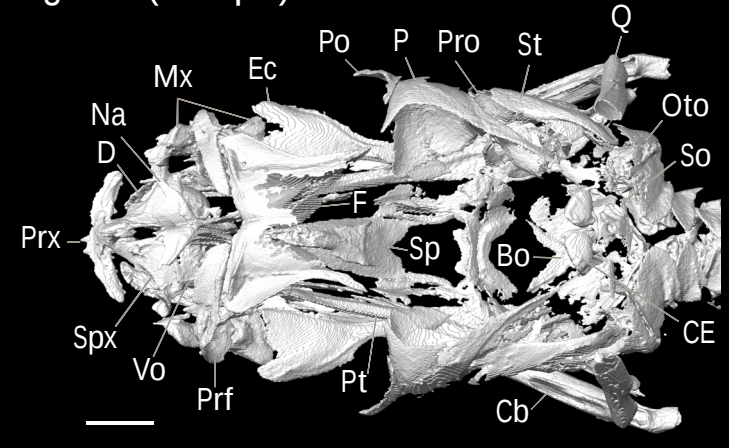

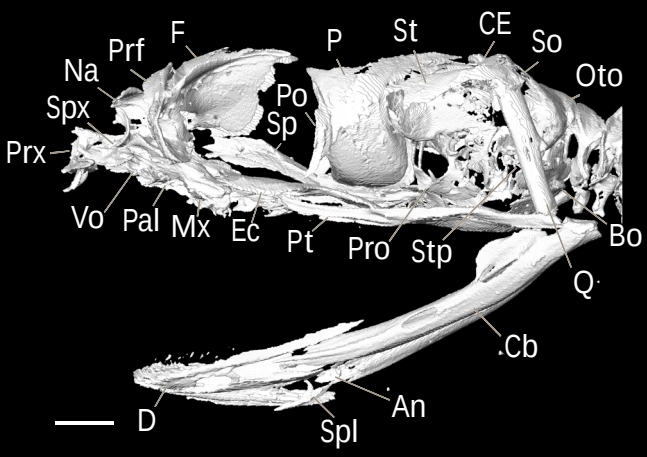

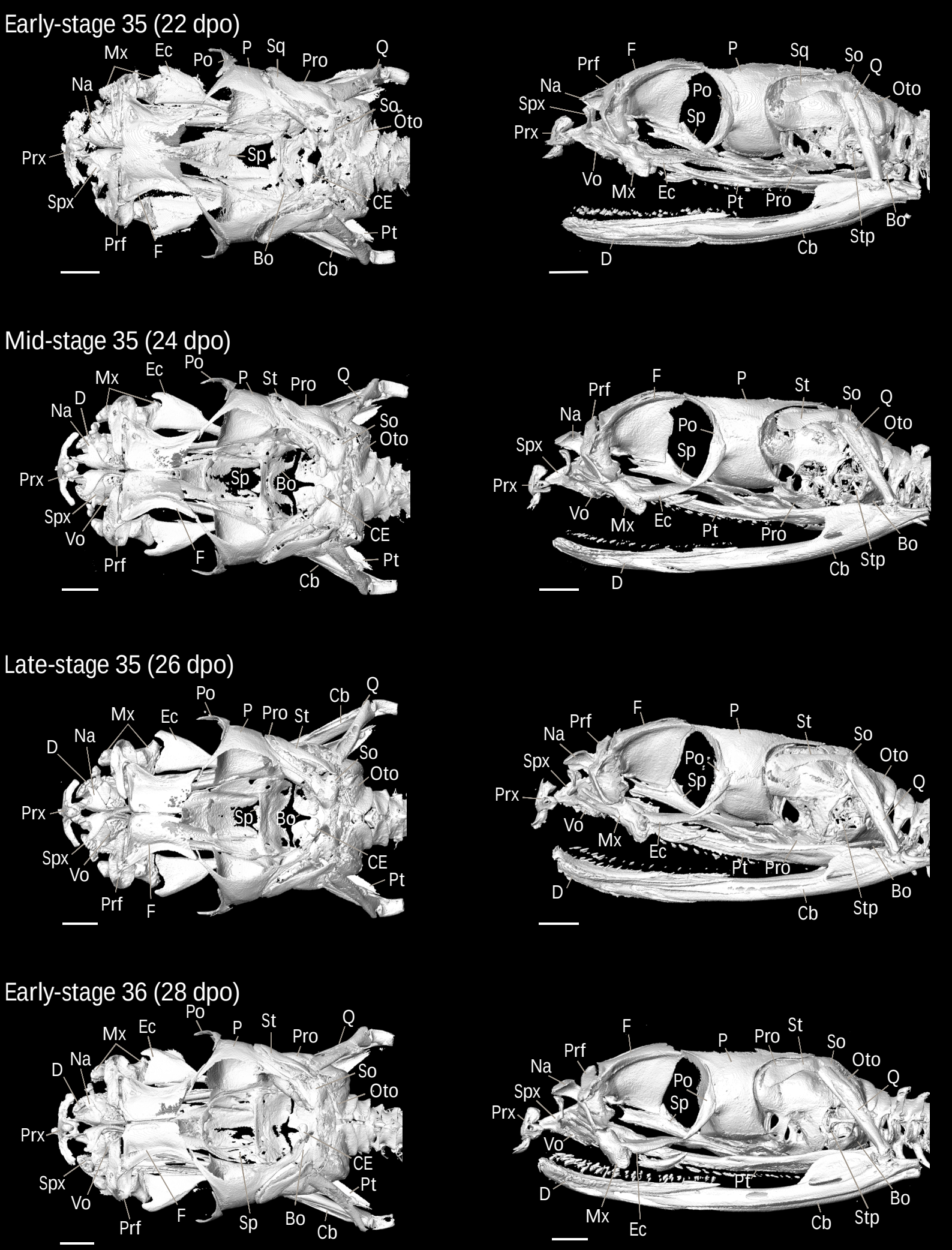
Early-stage 35 (22 dpo)
Mx
Ec
Po
P
Sq
Pro
Q
Na
So
Oto
Prx
Sp
Spx
CE
Pt
Prf
F
Bo
Cb
Vo
Stp
D
Mid-stage 35 (24 dpo)
St
Late-stage 35 (26 dpo)
Early-stage 36 (28 dpo)

Late-stage 36 (32 dpo)

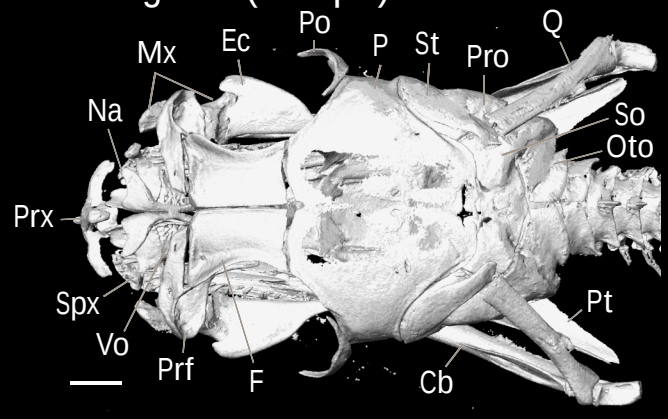

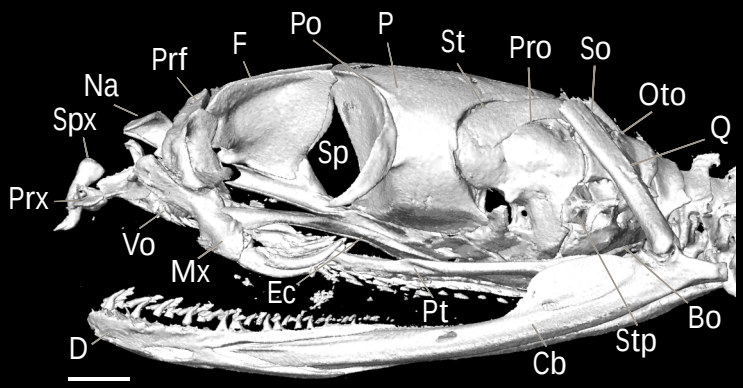

Stage 37 (35 dpo)

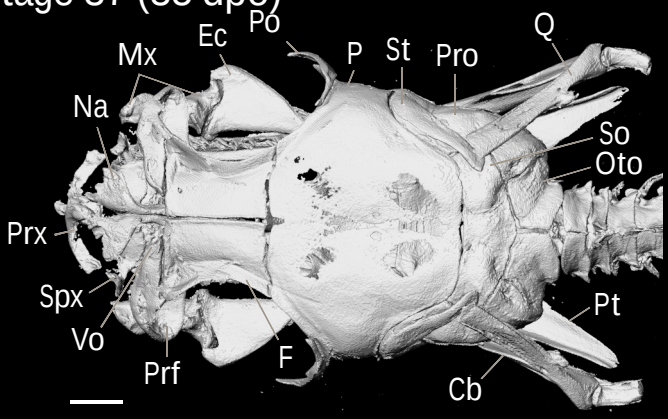

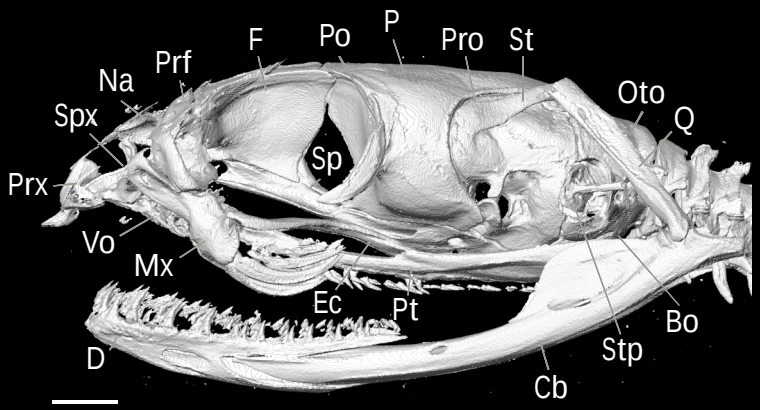

Stage 30

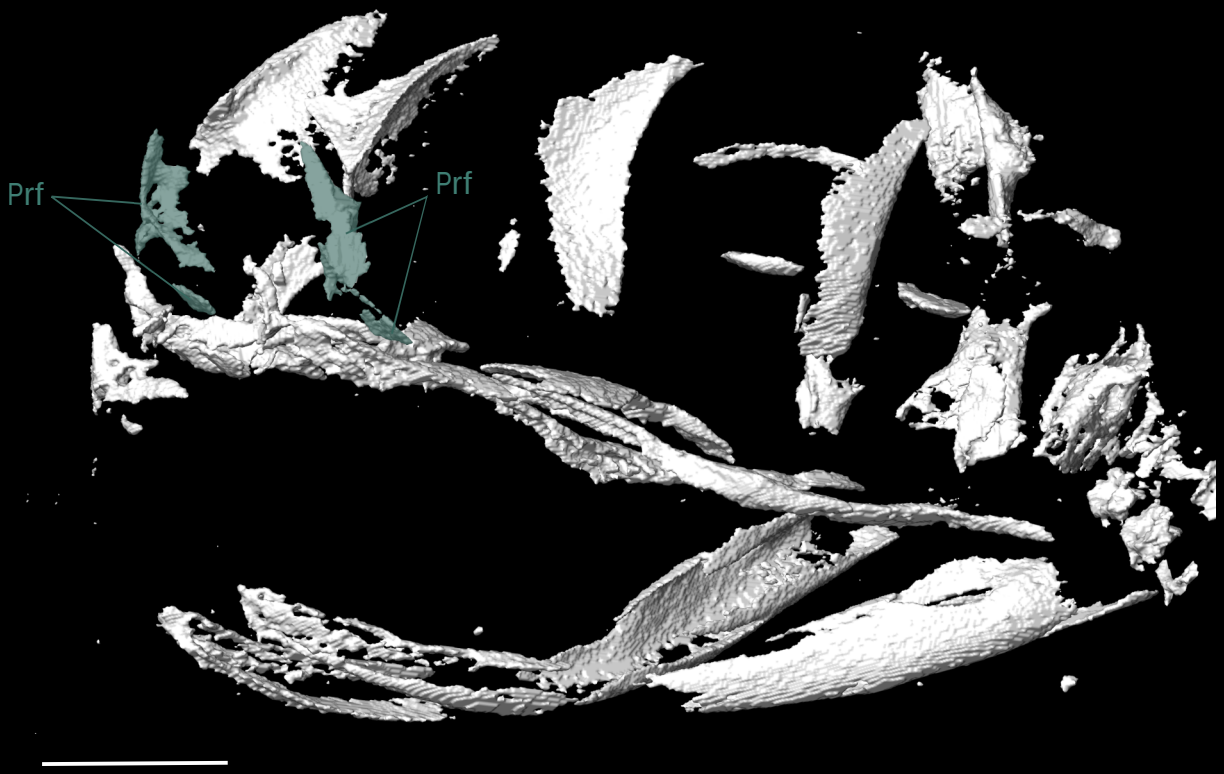

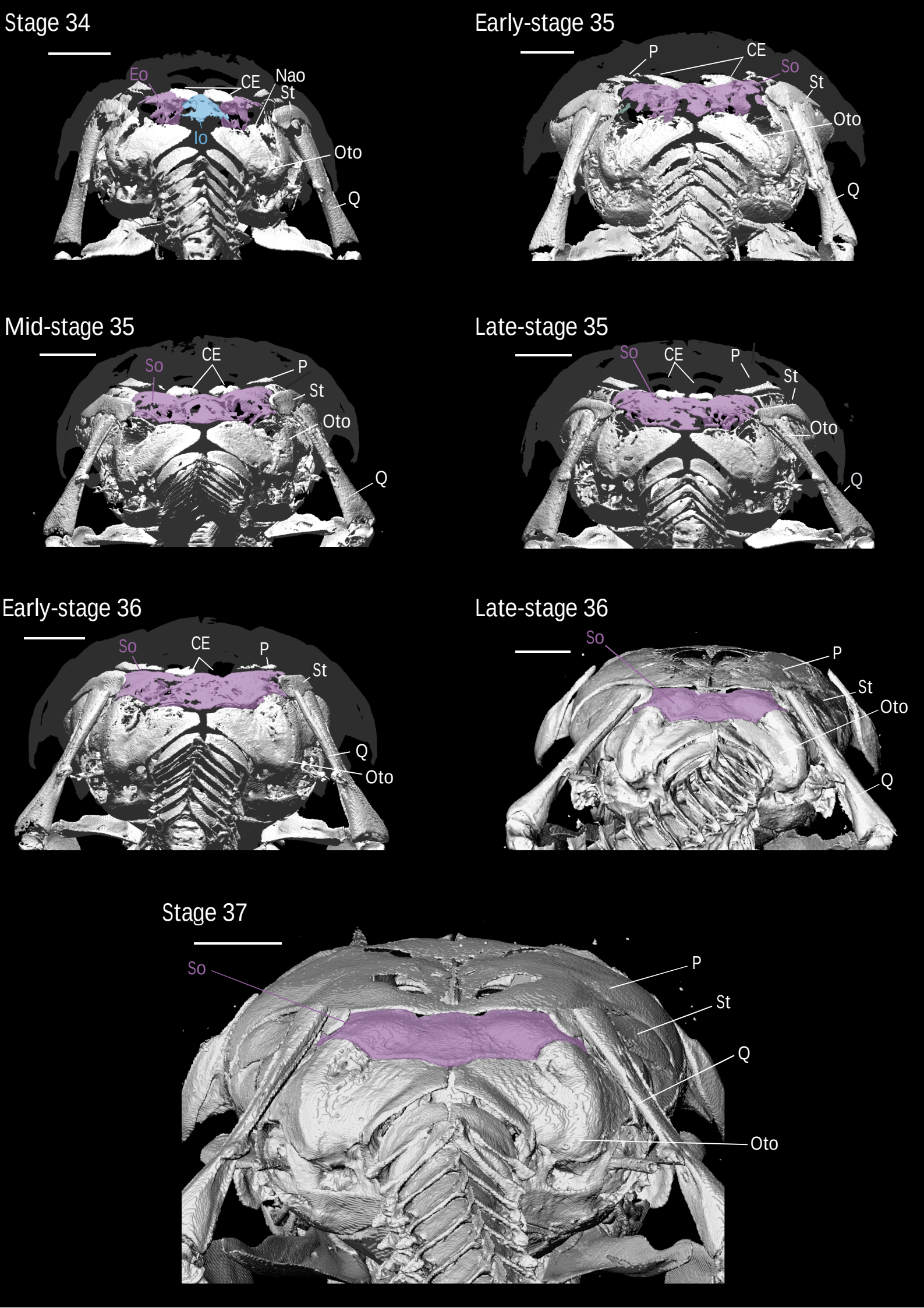
Stage 34
Eo
CE
Nao
St
Io
Oto
Q
Early-stage 35
P
CE
So
St
Oto
Q
Mid-stage 35
So
CE
P
St
Oto
Q
Late-stage 35
So
CE
P
St
Oto
Q
Early-stage 36
So
CE
P
St
Q
Oto
Late-stage 36
So
P
St
Oto
Q
Stage 37
So
P
St
Q
Oto

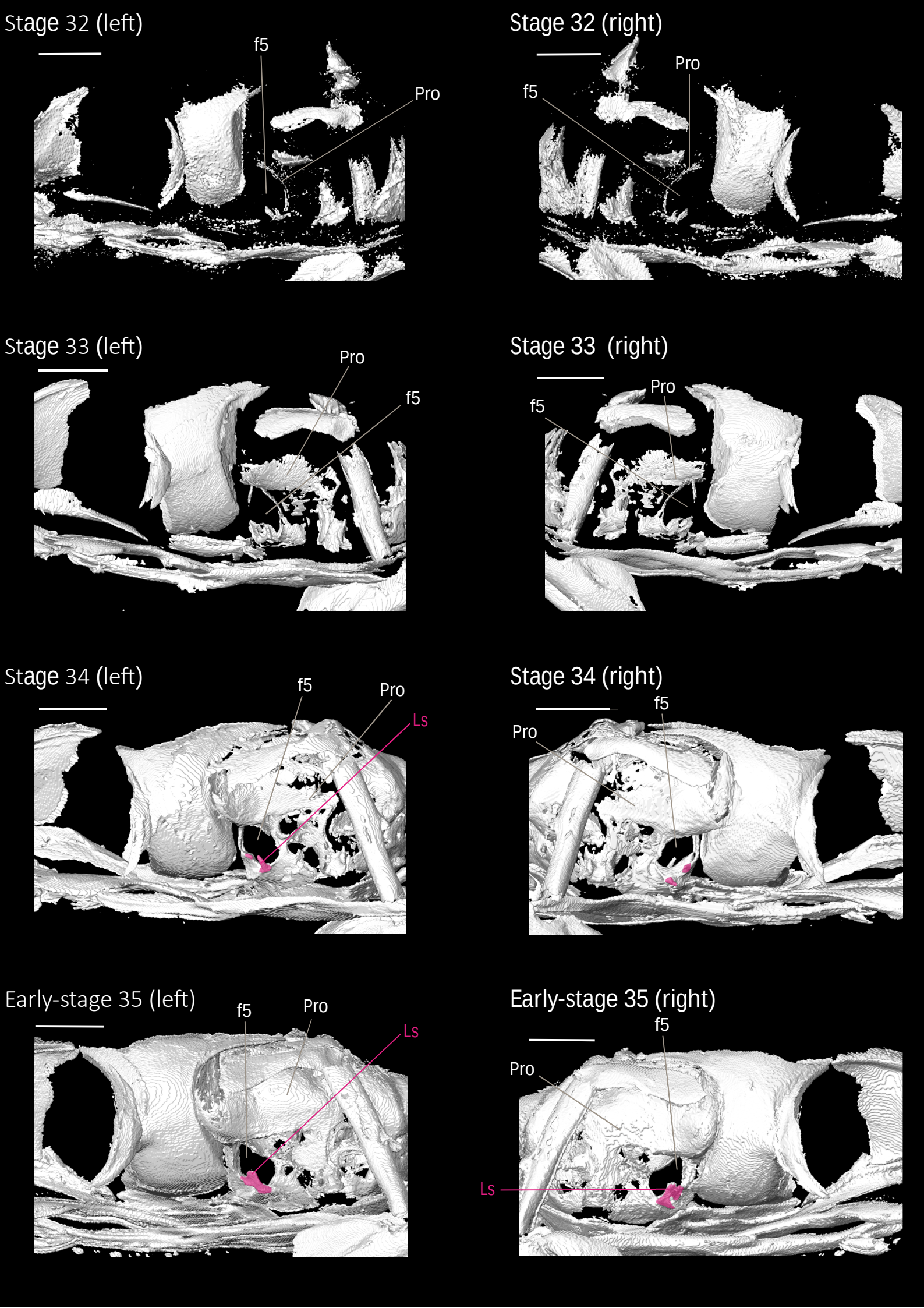
Stage 32 (left)
f5
Pro
Stage 32 (right)
Pro
f5
Stage 33 (left)
Pro
f5
Stage 33 (right)
Pro
f5
Stage 34 (left)
f5
Pro
Ls
Stage 34 (right)
f5
Pro
Early-stage 35 (left)
f5
Pro
Ls
Early-stage 35 (right)
f5
Pro
Ls

Mid-stage 35 (left)

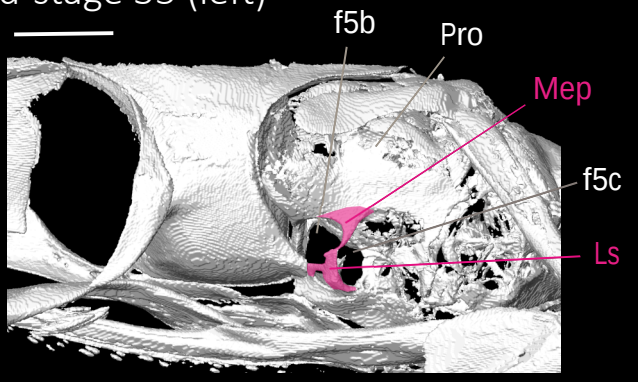

Mid-stage 35 (right)

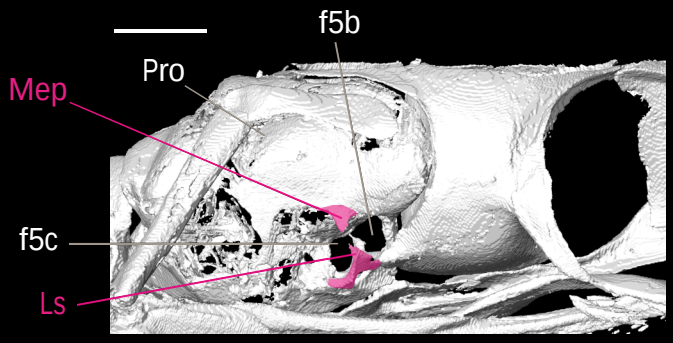

Early-stage 36 (left)

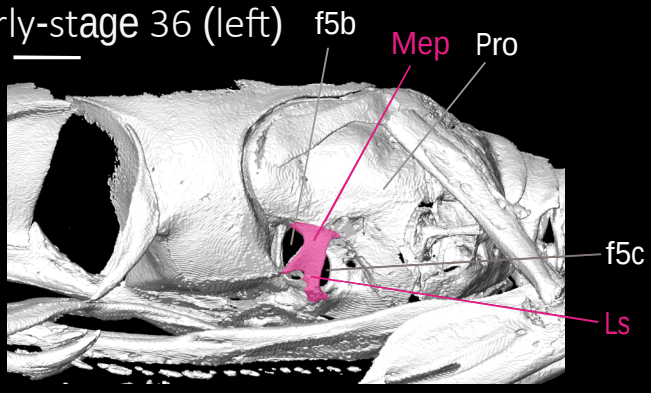

Early-stage 36 (right)

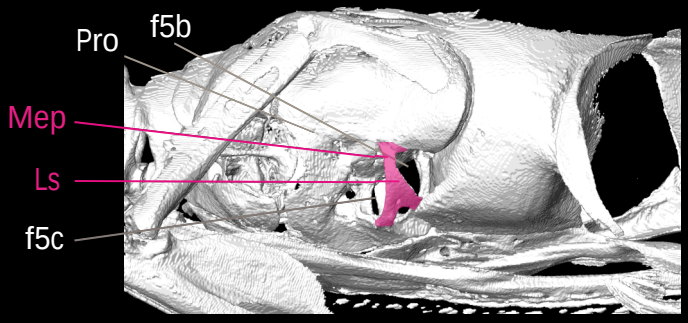

Late-stage 36 (left)

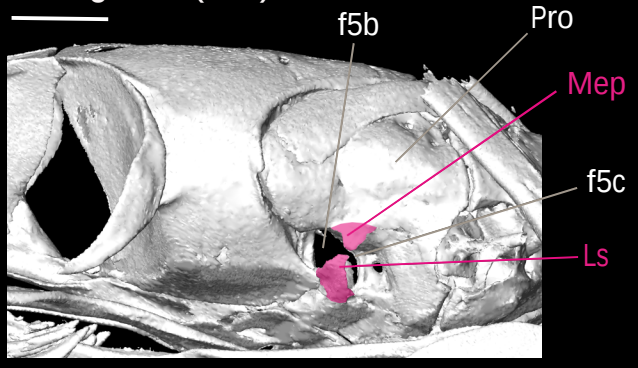

Late-stage 36 (right)

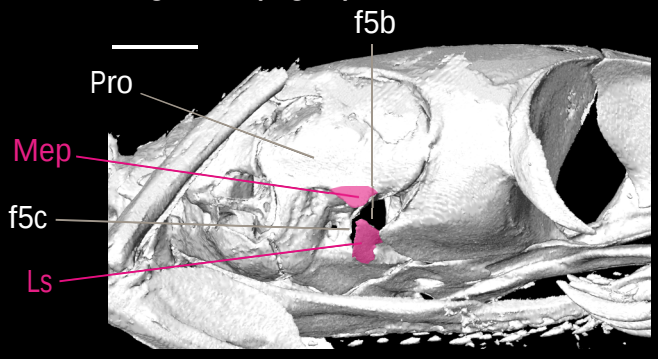

Stage 37 (left)

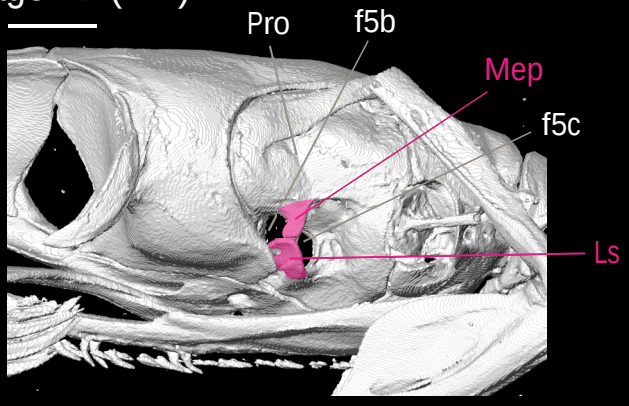

Stage 37 (right)